Chemical Science

Accepted Manuscript

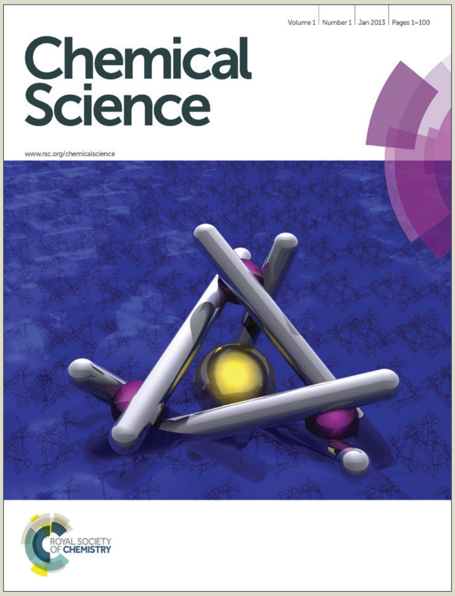

ROYAL SOCIETY
OF CHEMISTRY

www.rsc.org/chemicalscience

Cite this: DOI: 10.1039/c0xx00000x

www.rsc.org/xxxxxx

ARTICLE TYPE

Trapping of the Putative 1,2-Dinitrosoarene Intermediate of Benzofuroxan Tautomerization by Coordination at Ruthenium, and Exploration of its Redox Non-Innocence

Siu-Chung Chan,[a] Jason England,[b] Karl Wieghardt*[b] and Chun-Yuen Wong*[a]

Received (in XXX, XXX) Xth XXXXXXXXX 20XX, Accepted Xth XXXXXXXXX 20XX
DOI: 10.1039/b000000x

Reaction of benzofuroxans with [Ru([9]aneS3)(dmso)Cl_2] ([9]aneS3 = 1,4,7-trithiacyclononane) and $[Ru(bpy)_2(CH_3CN)_2]^{2+}$ yields the ruthenium complexes $[Ru([9]aneS3)(ON\text{^}NO)(Cl)]^+$ (**1a–1c**) and $[Ru(bpy)_2(ON\text{^}NO)]^{n+}$ (n = 2: **2a** and **2b**; n = 1: **2a**$^-$ and **2b**$^-$), respectively, containing neutral or monoanionic *N*,*N'*-coordinated 1,2-dinitrosoarenes (ON^NO). The oxidation states of the ON^NO ligands (0 for **1a**–**1c**, **2a** and **2b**; –1 for **2a**$^-$ and **2b**$^-$) have been deduced through detailed structural, spectroscopic, and theoretical studies. In other words, not only does this work demonstrate the trapping of the putative 1,2-dinitrosoarene intermediate of benzofuroxan tautomerization by coordination to ruthenium, it also provides access to a new family of redox-active bidentate ligand.

Benzofuroxans,[1,2] one of the most studied class of heterocyclic compounds in medicinal chemistry, are known to exhibit diverse bioactivities.[3-5] They undergo tautomerization, with transient 1,2-dinitrosoarenes believed to be formed as intermediates in the process (Scheme 1):[6-9]

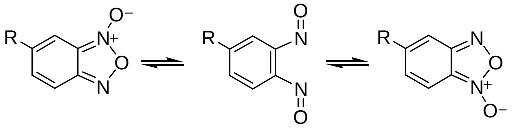

Scheme 1

The existence of these putative 1,2-dinitrosoarenes has been evidenced by kinetic studies,[10] theoretical calculations,[11,12] and formation of its chemical derivatives by reaction with *p*-anisyl azide and diphenyldiazomethane.[13] Trapping the transient 1,2-dinitrosoarene *itself* through metal complexation would not only strongly support the proposed tautomerization mechanism, but given that coordinated nitrosoarene can exist as either neutral, monoanionic, or dianionic ligand,[14,15] it may also provide a new family of ligands with redox non-innocent behavior.[16,17] More specifically, 1,2-dinitrosoarenes would be expected to behave in an analogous fashion to well-known bidentate *α*-diimine, dioxolenes and dithiolene redox-active ligand systems, which all exhibit rich redox chemistry,[18] and are known to play important roles in catalysis,[19] material research[20] and bioinorganic chemistry.[21] In this study, we confirm this to be the case via the synthesis, spectroscopic characterization, and theoretical calculations of two series of ruthenium complexes, one with neutral 1,2-dinitrosoarenes $(ON\text{^}NO)^0$ and the other with monoanionic 1,2-dinitrosoarene radicals $(ON\text{^}NO)^{\bullet-}$. Although the chemistry of 1,2-dinitrosoalkane and 1,2-dinitrosoalkene complexes is well developed (no evidence has been presented of redox non-innocence),[22] these complexes are the first examples of isolable and structurally characterized metal 1,2-dinitrosoarene complexes.

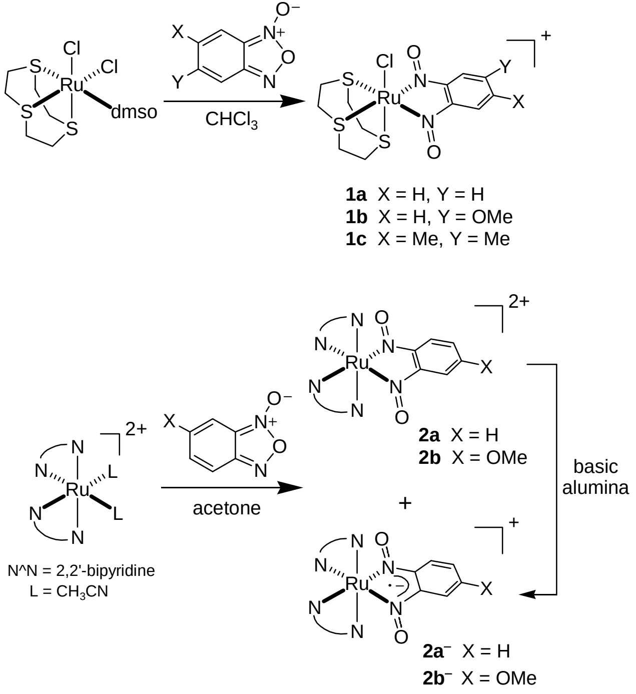

Scheme 2

Diamagnetic complexes $[Ru([9]aneS3)(ON\text{^}NO)^0(Cl)]^+$ (**1a**–**1c**) were cleanly prepared by reaction of [Ru([9]aneS3)(dmso)Cl_2] with benzofuroxans (Scheme 2). In contrast, reacting $[Ru(bpy)_2(CH_3CN)_2]^{2+}$ with benzofuroxans did not lead to a single product, but a mixture of diamagnetic $[Ru(bpy)_2(ON\text{^}NO)^0]^{2+}$ (**2a**, **2b**) and paramagnetic

$[Ru(bpy)_2(ON^\wedge NO)^{\bullet-}]^+$ (**2a**⁻, **2b**⁻). However, it was found that complexes **2a** and **2b** could be reduced by basic alumina chromatographic treatment, thereby yielding **2a**⁻ and **2b**⁻ as the sole products.

The oxidation states of the ON^NO ligands (0 for **1a**–**1c**, **2a** and **2b**; –1 for **2a**⁻ and **2b**⁻) have been deduced through detailed structural, spectroscopic, and theoretical studies. Firstly, the ν_{NO} stretching frequencies for the diamagnetic complexes **1a**–**1c**, **2a** and **2b** fall in the narrow range 1365–1389 cm^{-1}, and are approximately 150 cm^{-1} higher in energy than those for the paramagnetic complexes **2a**⁻ and **2b**⁻ (1218–1239 cm^{-1}). This implies a significant weakening of the N–O bond upon reduction, which is indicative of predominantly ligand-centered reduction. The X-ray crystal structures determined for **1a**, **1b**, **2b**, **2a**⁻ and **2b**⁻ (Fig 1 and S2–S5; Table 1 and S1) further support this nation, with the N–O distances in **1a**, **1b** and **2b** (1.227(5)–1.243(3) Å) being significantly shorter than those in **2a**⁻ and **2b**⁻ (1.265(5)–1.274(4) Å). Interestingly, the Ru–N_{NO} bonds also decrease in length upon reduction, from 1.930(3)–1.966(2) to 1.975(3)–2.000(4) Å, presumably due to a diminished ligand π-acceptor capacity in its reduced state.

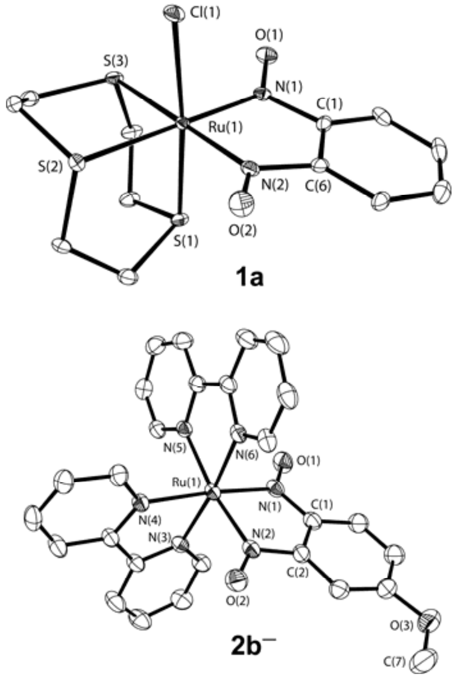

Fig. 1 Perspective view of **1a** and **2b**⁻ depicted using 30% probability ellipsoids. Hydrogen atoms have been omitted for clarity.

Table 1 Selected bond lengths (Å) and angles (°) for **1a**, **1b**, **2b**, **2a**⁻ and **2b**⁻

complex	**1a**[a]	**1b**[a]	**2b**	**2a**⁻	**2b**⁻
Ru–N_{NO}	1.945(5)–1.950(3)	1.956(2)–1.966(2)	1.930(3), 1.956(3)	1.975(3), 1.989(3)	1.982(4), 2.000(4)
N–O	1.227(5)–1.234(5)	1.227(3)–1.243(3)	1.230(4), 1.241(4)	1.272(5), 1.274(4)	1.265(5), 1.265(5)
N_{NO}–C	1.424(6)–1.451(6)	1.418(3)–1.448(3)	1.459(4), 1.420(4)	1.383(6), 1.399(5)	1.382(6), 1.383(6)
C_{NO}–C_{NO}	1.393(7), 1.403(7)	1.396(3), 1.400(3)	1.395(5)	1.421(6)	1.415(7)
N_{NO}–Ru–N_{NO}	83.22(15), 83.27(15)	82.46(8), 82.54(8)	83.32(12)	81.55(14)	81.34(16)

[a] The crystal contains two crystallographically independent cations in the asymmetric unit.

Within the spectral guidelines forwarded by Tomson and co-workers[14] for assigning oxidation states of nitrosoarene (PhNO) ligands bound to transition metal ions, complexes may contain η^1-bound neutral ligands $(PhNO)^0$ with (1) little π-backbonding (d_{NO} = 1.20–1.23 Å, and ν_{NO} = 1400–1500 cm^{-1}) or (2) considerable metal-to-ligand π-backbonding (d_{NO} = 1.23–1.26 Å, and ν_{NO} = 1300–1400 cm^{-1}). They may also possess redox states that are best defined as (3) η^1-$(PhNO)^{\bullet-}$ radical anions (d_{NO} = 1.26–1.31 Å, and ν_{NO} = 1150–1300 cm^{-1}) or (4) η^2-$(PhNO)^{2-}$ dianions (d_{NO} > 1.32 Å, and ν_{NO} = 900–1150 cm^{-1}). Based upon their spectral parameters, complexes **1a**–**1c**, **2a** and **2b** fall within category 2, associated with η^1-$(PhNO)^0$ possessing strong metal-to-ligand π-backbonding, whereas those for **2a**⁻ and **2b**⁻ are consistent with expectations for a η^1-$(PhNO)^{\bullet-}$ ligand (category 3). These conclusions are consistent with our own experimental results and suggest that the aforementioned redox assignment guidelines for nitrosoarene ligands may be equally valid for dinitrosoarenes.

To rationalize the structural and spectroscopic difference between these two classes of complexes, density functional theory (DFT) calculations were performed. The ground state structures of $S = 0$ **1a**–**1c**, **2a**, **2b** (referred to in a generic sense as **1** and **2**) and their $S = 1/2$ one-electron reduced forms **1a**⁻–**1c**⁻, **2a**⁻, **2b**⁻ (referred to in a generic sense as **1**⁻ and **2**⁻) reproduce the observed Ru–N_{NO} and N–O distances. For example, the calculated Ru–N_{NO} and N–O distances are 1.96–1.98 and 1.23 Å respectively in **1** and **2**, and they are 1.99–2.01 and 1.26–1.27 Å respectively in **1**⁻ and **2**⁻ (Fig. 2). The frontier molecular orbitals compositions of **1**–**2** (Table 2) clearly show that their lowest unoccupied molecular orbitals (LUMOs) have significant ON^NO contribution (77–82%), signifying a ligand-based reduction. The structural changes from **1**/**2** to **1**⁻/**2**⁻ can be readily understood based upon the nature of the LUMOs of the former: the surface plots for the LUMOs of **1a** and **2a** (Fig. 3) clearly show that these π(ON^NO)-based LUMOs are π-antibonding with respect to the Ru–N_{NO} and N–O bonds, and populating these orbitals would therefore lead to elongation of these bonds. Similarly, the shorter N_{NO}–C and longer C_{NO}–C_{NO} distances in **1**⁻ and **2**⁻ compared with **1** and **2**, observed both experimentally and theoretically, can also be explained by the respective π-bonding and π-antibonding nature of these bonds in the LUMOs of **1** and **2**.

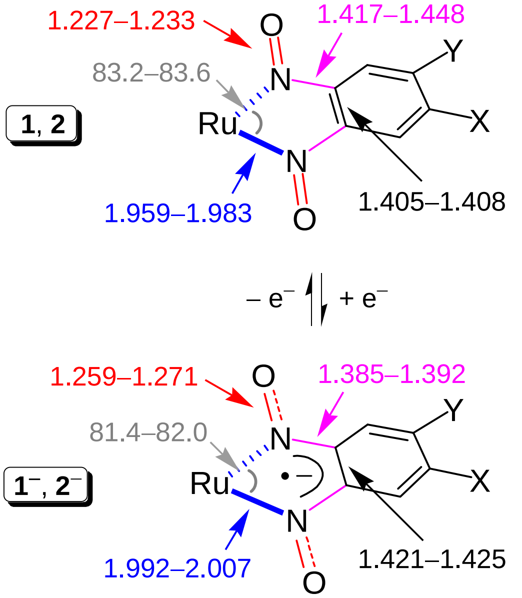

Fig. 2 Selected bond lengths (Å) and angles (°) of the DFT geometry optimized structures. Ligands other than ON^NO are omitted for clarity.

Table 2 Frontier molecular orbital composition (%) of **1**–**2**

complex	MO	Ru	ON^NO	[9]aneS3	Cl	2 × bpy
1a	HOMO	38.95	16.82	16.68	27.55	–
	LUMO	12.80	81.80	4.60	0.80	–
1b	HOMO	39.20	24.30	14.31	22.19	–
	LUMO	12.83	81.69	4.72	0.76	–
1c	HOMO	39.88	19.52	16.18	24.42	–
	LUMO	12.43	82.25	4.58	0.74	–
2a	HOMO	62.86	13.45	–	–	23.69
	LUMO	12.12	77.29	–	–	10.59
2b	HOMO	61.95	16.95	–	–	21.10
	LUMO	12.10	76.62	–	–	11.28

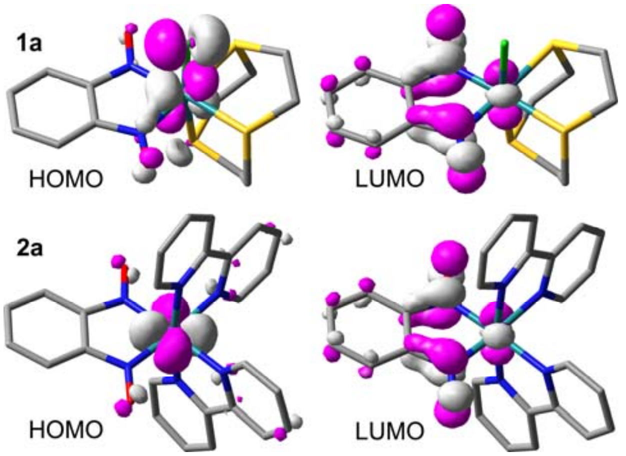

Fig. 3 Surface plots of the HOMO and LUMO of **1a** and **2a** (surface isovalue = 0.06 au) taken from DFT calculations.

The X-band EPR spectra of **2a**$^-$ and **2b**$^-$, recorded at room temperature, show signals consistent with $S = 1/2$ electronic ground states (Table 3). The narrow linewidths and narrow distribution of g-values that do not diverge greatly from that of the free electron suggest that the unpaired electron is in both cases ligand-centered. The EPR spectrum of **2b**$^-$ has a more complex hyperfine structure than **2a**$^-$ (Fig. 4), with the former displaying two distinct ^{14}N-hyperfine coupling constants ($A_{\text{iso}}\{^{14}\text{N}\} = 2.5 \times 10^{-4}$ and 4.3×10^{-4} cm^{-1}), and the latter displaying a hyperfine interaction with two chemically equivalent ^{14}N-atoms. This reflects the asymmetry of the ON^NO ligand in **2b**$^-$ due to the presence of methoxy substituent, and confirms that the unpaired electron is localized on the ON^NO, rather than on the bpy ligand. The room temperature EPR spectra of electrochemically generated **1b**$^-$ and **1c**$^-$ (see ESI) display similar, but more poorly resolved hyperfine coupling patterns. Their spectra are once again consistent with the unpaired electron residing on the ON^NO ligand, which is confirmed in **1b** by observation of a hyperfine interaction to two chemically distinct ^{14}N-atoms.

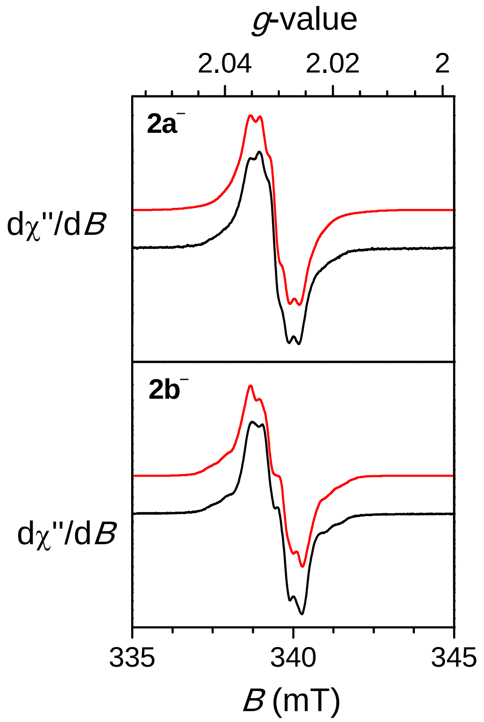

Fig. 4 Perpendicular mode X-band EPR spectrum (black line) and spectral simulation (red line) of **2a**$^-$ and **2b**$^-$ recorded in CH_2Cl_2 solution at room temperature. Conditions: frequency 9.65 GHz; power 2.0 mW; modulation 0.005 mT for **2a**$^-$ and 0.03 mT for **2b**$^-$. Simulations were performed using the parameters listed in Table 3.

Table 3 EPR spectroscopic parameters for **1b**$^-$, **1c**$^-$, **2a**$^-$ and **2b**$^-$

complex	g_{iso}	$A_{\text{iso}}\{^{14}\text{N}\}$, 10^{-4} cm^{-1}	$A_{\text{iso}}\{^{101}\text{Ru}, {}^{99}\text{Ru}\}$, 10^{-4} cm^{-1}
1b$^-$	2.032	4.2, 2.5	3.2
1c$^-$	2.032	3.1	2.4
2a$^-$	2.031	3.1	2.7
2b$^-$	2.031	4.3, 2.5	4.3

Consistent with the EPR findings, the calculated Löwdin spin densities for both **1**$^-$ and **2**$^-$ are localized mainly on the ON^NO ligands with populations close to 1 electron (Fig. 5). Note that in **1b**$^-$ and **2b**$^-$ the spin density distributions over the ON^NO moieties are asymmetric (spin populations for the two N atoms are 0.13 and 0.20 in **1b**$^{-}$, and 0.12 and 0.19 in **2b**$^{-}$), consistent with their EPR spectra both featuring two distinct $A_{\mathrm{iso}}\{^{14}\mathrm{N}\}$-values. Based upon the aforementioned structural, spectral, and theoretical studies, the ON^NO ligands in **2a**$^{-}$ and **2b**$^{-}$ can be confidently assigned as being monoanionic 1,2-dinitrosoarene radicals (ON^NO)$^{\bullet-}$, whereas those in **1a**–**1c**, **2a** and **2b** correspond to neutral (ON^NO)^{0} ligands.

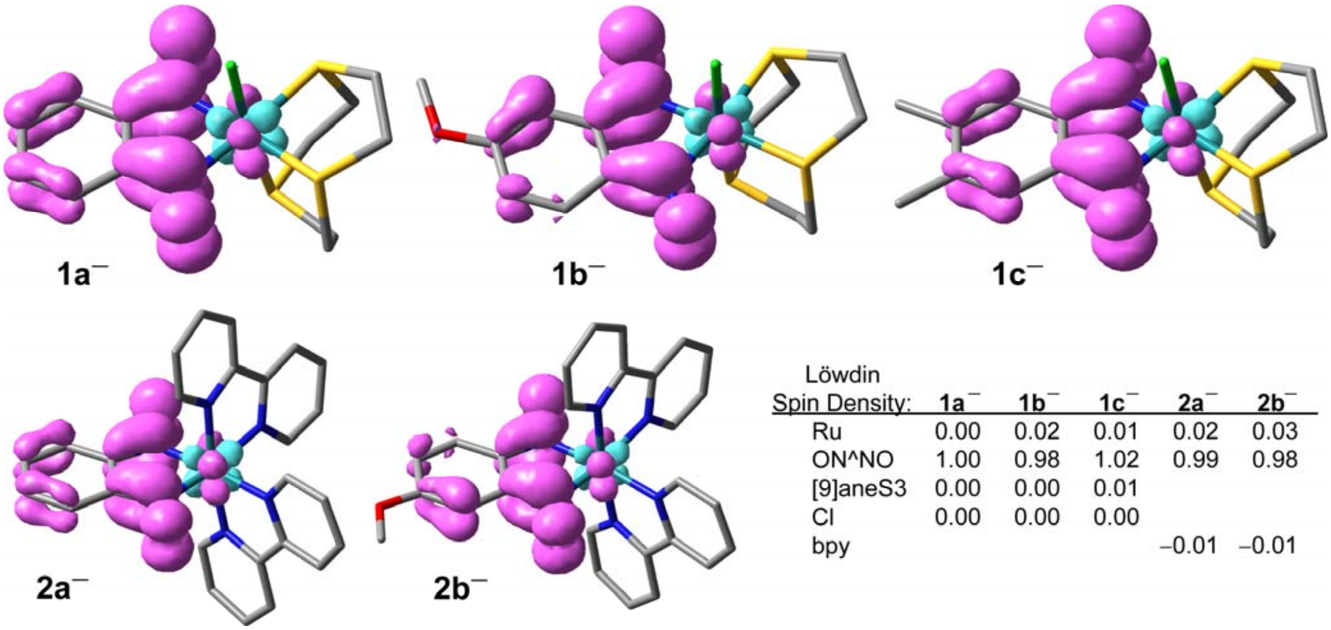

Löwdin Spin Density:	1a⁻	1b⁻	1c⁻	2a⁻	2b⁻
Ru	0.00	0.02	0.01	0.02	0.03
ON^NO	1.00	0.98	1.02	0.99	0.98
[9]aneS3	0.00	0.00	0.01		
Cl	0.00	0.00	0.00		
bpy				–0.01	–0.01

Fig. 5 Löwdin spin density distribution in **1**$^{-}$ and **2**$^{-}$ (surface isovalue = 0.002 au) taken from DFT calculations. Positive and negative spin densities are shown in pink and cyan, respectively.

Last but not least, the ON^NO-ligated complexes exhibit two reversible redox couples in the range of 0.0 to –1.1 V vs Fc$^{+/0}$ (Table 4). The first, found between –0.13 to –0.30 V versus Fc$^{+/0}$, correspond to the ligand-centered ON^NO$^{0/\bullet-}$ couples, and the second (–0.86 to –1.05 V) are tentatively assigned as belonging to ON^NO$^{\bullet-/2-}$ redox couples. These potentials are significantly less negative than those in the nitrosoarene-centered reductions reported for the complexes [Ru([9]aneS3)(ON^N)(CH$_3$CN)]$^{2+}$ and [Ru([14]aneS4)(PhNO)Cl]$^{+}$ (–0.67 and –0.94 V respectively; ON^N = 2-(2-nitrosophenyl)pyridine, [14]aneS4 = 1,4,8,11-tetrathiacyclotetradecane).[15a,b], and the bpy-centered reduction in [Ru(bpy)$_3$]$^{2+}$ (–1.76 V).[23]

In conclusion, we have trapped the putative 1,2-dinitrosoarene intermediate of benzofuroxan tautomerization by coordination to ruthenium. Moreover, the *N*,*N*'-coordinated 1,2-dinitrosoarenes represent a new class of redox-active bidentate ligand, for which ruthenium complexes bearing neutral (ON^NO)^{0} or monoanionic radical (ON^NO)$^{\bullet-}$ have been isolated and structurally characterized. The aforementioned redox processes occur at mild potentials, so provide easy access to reduced ligand states. The neutral (ON^NO)^{0} and the monoanionic radical (ON^NO)$^{\bullet-}$ are structurally and spectroscopically distinct, hence this work also provides a benchmark for further exploration of these ligands. The isolation/characterization of ON^NO^{2-}-ligated species, and the development of functional molecular electronics and catalysts based on the ON^NO-ligated complexes are currently under investigation in our laboratory.

Table 4 Electrochemical data[a]

complex	$E_{1/2}$[b]/V vs Fc$^{+/0}$	
	1st reduction	2nd reduction
1a	–0.24	–0.99
1b	–0.27	–1.00
1c	–0.30	–1.05
2a	–0.13	–0.86
2b	–0.17	–0.90
[Ru([9]aneS3)(ON^N)(CH$_3$CN)]$^{2+}$	–0.67	–1.69[c]
[Ru([14]aneS4)(PhNO)Cl]$^{+}$	–0.94	–1.98[d]

[a]Supporting electrolyte: 0.1 M [Bu$_4$N]PF$_6$ in CH$_3$CN. [b]$E_{1/2}$ = (E_{pc} + E_{pa})/2 at 298 K for reversible couples. [c]Quasi-reversible; the recorded potential is the cathodic potential at scan rate of 100 mV s^{-1}. [d]Irreversible.

Acknowledgement

The work described in this paper was supported by grants from the Hong Kong Research Grants Council (Project No. CityU 103911) and City University of Hong Kong (Project No. 7004022), and by the Max Planck Society who granted J.E. a fellowship. We are grateful to Dr. Shek-Man Yiu for X-ray diffraction data collection.

Notes and references

[a] *Department of Biology and Chemistry, City University of Hong Kong, Tat Chee Avenue, Kowloon, Hong Kong SAR, People's Republic of China. E-mail: acywong@cityu.edu.hk*

[b] *Max-Planck-Institut für Chemische EnergieKonversion, Stiftstrasse 34–36, 45470 Mülheim an der Ruhr, Germany.E-mail: karl.wieghardt@cec.mpg.de*

† Electronic Supplementary Information (ESI) available: Experimental procedures and characterization data, spectroscopic data, theoretical calculation details, crystallographic data in CIF format (CCDC 994514–994518). See DOI: 10.1039/b000000x/

1 A. J. Boulton and P. B. Ghosh, *Advances in Heterocyclic Chemistry, vol. 10*, Academic Press: New York, 1969, 1.

2 R. J. Gaughran, J. P. Picard and J. V. R. Kaufman, *J. Am. Chem. Soc.,* 1954, **76**, 2233.

3 H. Cerecetto and M. González, *Benzofuroxan and Furoxan. Chemistry and Biology, Top. Heterocycl. Chem., Bioactive Heterocycle IV*, Springer: Berlin/Heidelberg, 2007, **10**, 265-308.

4 P. G. Wang, M. Xian, X. Tang, X. Wu, Z. Wen, T. Cai and A. J. Janzcuk, *Chem. Rev.,* 2002, **102**, 1091.

5 C. Jovene, E. A. Chugunova and R. Goumont, *Mini. Rev. Med. Chem.,* 2013, **13**, 1089.

6 J. H. Boyer, U. Toggweiler and G. A. Stoner, *J. Am. Chem. Soc.,* 1957, **79**, 1748.

7 B. G. Gowenlock and G. B. Richter-Addo, *Chem. Soc. Rev.,* 2005, **34**, 797.

8 I. R. Dunkin, M. A. Lynch, A. J. Boulton and N. Henderson, *Chem. Commun.,* 1991, 1178.

9 N. P. Hacker, *J. Org. Chem.,* 1991, **56**, 5216.

10 *(a)* F. B. Mallory, S. L. Manatt and C. S. Wood, *J. Am. Chem. Soc.,* 1965, **87**, 5433; *(b)* F. B. Mallory and A. Cammarata, *J. Am. Chem. Soc.,* 1966, **88**, 61.

11 W. Friedrichsen, *J. Phys. Chem.,* 1994, **98**, 12933.

12 J. Stevens, M. Schweizer and G. Rauhut, *J. Am. Chem. Soc.,* 2001, **123**, 7326.

13 A. B. Bulacinski, E. F. V. Sciven and H. Suschitzky, *Tetrahedron Lett.*, 1975, 3577.

14 N. C. Tomson, L. A. Labios, T. Weyhermüller, J. S. Figueroa and K. Wieghardt, *Inorg. Chem.*, 2011, **50**, 5763.

15 *(a)* S.-C. Chan, P.-K. Pat, T.-C. Lau and C.-Y. Wong, *Organometallics,* 2011, **30**, 1311; *(b)* S.-C. Chan, H.-Y. Cheung and C.-Y. Wong, *Inorg. Chem.,* 2011, **50**, 11636; *(c)* S.-C. Chan, J. England, W.-C. Lee, K. Wieghardt and C.-Y. Wong, *ChemPlusChem,* 2013, **78**, 214.

16 C. K. Jørgensen, *Coord. Chem. Rev.* 1966, **1**, 164.

17 P. J. Chirik and K. Wieghardt, *Science*, 2010, **327**, 794.

18 For recent reviews and special issues on non-innocent ligands, see: *(a)* "Dithiolenes and non-innocent redox-active ligands: COST Action D35 Conference 2009", *Coord. Chem. Rev.,* 2010, **254**, issue 13-14; *(b)* "Forum on Redox-Active Ligands", *Inorg. Chem.,* 2011, **50**, 9737-9914; *(c)* "Special Issue: Cooperative & Redox Non-Innocent Ligands in Directing Organometallic Reactivity (Cluster Issue, Guest Editor: Bas De Bruin)", *Eur. J. Inorg. Chem.*, 2012, issue 3.

19 *(a)* A. M. Allgeier and C. A. Mirkin, *Angew. Chem., Int. Ed.,* 1998, *37*, 894; *(b)* T. Wada, K. Tsuge and K. Tanaka, *Angew. Chem., Int. Ed.,* 2000, **39**, 1479; *(c)* V. Lyaskovskyy and B. de Bruin, *ACS Catal.,* 2012, **2**, 270; *(d)* O. R. Luca and R. H. Crabtree, *Chem. Soc. Rev.,* 2013, **42**, 1440.

20 *(a)* A. T. Coomber, D. Beljonne, R. H. Friend, J. L. Brédas, A. Charlton, N. Robertson, A. E. Underhill, M. Kurmoo and P. Day, *Nature,* 1996, **380**, 144; *(b)* H. Tanaka, Y. Okano, H. Kobayashi, W. Suzuki and A. Kobayashi, *Science*, 2001, **291**, 285; *(c)* N. Robertson and L. Cronin, *Coord. Chem. Rev.,* 2002, **227**, 93; *(d)* A. Dei, D. Gatteschi, C. Sangregorio and L. Sorace, *Acc. Chem. Res.,* 2004, **37**, 827; *(e)* R. Kato, *Chem. Rev.,* 2004, **104**, 5319.

21 *(a)* R. Hille, *Chem. Rev.,* 1996, **96**, 2757; *(b)* M. K. Johnson, D. C. Rees and M. W. W. Adams, *Chem. Rev.,* 1996, **96**, 2817; *(c)* W. Kaim and B. Schwederski, *Coord. Chem. Rev.,* 2010, **254**, 1580.

22 For related dinitrosoalkane/dinitrosoalkene complexes, see: *(a)* H. Brunner and S. Loskot, *Angew. Chem., Int. Ed.,* 1971, **10**, 515; *(b)* G. Evrard; R. Thomas, B. R. Davis and I. Bernal, *J. Organomet. Chem.* 1977, **124**, 59; *(c)* P. N. Becker, M. A. White and R. G. Bergman, *J. Am. Chem. Soc.,* 1980, **102**, 5676; *(d)* P. N. Becker and R. G. Bergman, *J. Am. Chem. Soc.*, 1983, **105**, 2985; *(e)* P. N. Becker and R. G. Bergman, *Organometallics*, 1983, **2**, 787; *(f)* W.-H. Chiu, K.-K. Cheung and C.-M. Che, *Chem. Commun.,* 1995, 441; *(g)* K. V. Luzyanin, P. V. Gushchin, A. J. L. Pombeiro, M. Haukka, V. I. Ovcharenko and V. Y. Kukushkin, *Inorg. Chem.,* 2008, **47**, 6919; *(h)* J. M. Schomaker, W. C. Boyd, I. C. Stewart, F. D. Toste and R. G. Bergman, *J. Am. Chem. Soc.*, 2008, **130**, 3777; *(i)* J. M. Schomaker, F. D. Toste and R. G. Bergman, *Org. Lett.,* 2009, **11**, 3698; *(j)* O. Das, S. Paria, E. Zangrando and T. K. Paine, *Inorg. Chem.*, 2011, **50**, 11375; *(k)* M. R. Crimmin, R. G. Bergman and F. D. Toste, *Angew. Chem., Int. Ed.,* 2011, **50**, 4484; *(l)* M. R. Crimmin, L. E. Rosebrugh, N. C. Tomson, T. Weyhermüller, R. G. Bergman, F. D. Toste and K. Wieghardt, *J. Organomet. Chem.*, 2011, **696**, 3974; *(m)* C. Zhao, M. R. Crimmin, F. D. Toste and R. G. Bergman, *Acc. Chem. Res.*, 2014, **47**, 517.

23 A. Juris, V. Balzani, F. Barigelletti, S. Campagna, P. Belser and A. von Zelewsky, *Coord. Chem. Rev.,* 1988, **84**, 85.